

## Rapid, Reversible Heterolytic Cleavage of Bound H<sub>2</sub>

Elliott B. Hulley, Kevin D. Welch, Aaron M. Appel, Daniel L. DuBois, and R. Morris Bullock\*

Center for Molecular Electrocatalysis, Physical Sciences Division, Pacific Northwest National Laboratory, P.O. Box 999, K2-57, Richland, Washington 99352, United States

**S** Supporting Information

**ABSTRACT:** Heterolytic cleavage of dihydrogen into a proton and a hydride ion is a fundamentally important step in many reactions, including the oxidation of hydrogen by hydrogenase enzymes and ionic hydrogenation of organic compounds. We report the facile, *reversible* heterolytic cleavage of H<sub>2</sub> in a manganese complex bearing a pendant amine, leading to the formation of a manganese hydride and a protonated amine that undergo H<sup>+</sup>/H<sup>-</sup> exchange at an estimated rate of >10<sup>7</sup> s<sup>-1</sup> at 25 °C.

The H–H bond of dihydrogen is the simplest chemical bond and has served as the prototypical bond for fundamental experimental and theoretical studies. The formation and cleavage of H<sub>2</sub> can occur homolytically (H·/H·) or heterolytically (H<sup>+</sup>/H<sup>-</sup>) and is an essential step in many reactions, including the production of H<sub>2</sub>,<sup>1</sup> the oxidation of H<sub>2</sub>,<sup>2</sup> and catalytic hydrogenation of a diverse range of unsaturated bonds.<sup>3</sup> In polar environments, typical of enzymatic or electrochemical reactions, the heterolytic bond strength for H–H cleavage<sup>4</sup> is lower than the homolytic bond strength, favoring heterolytic scission. Bifunctional interactions that facilitate the heterolysis of H<sub>2</sub> (Figure 1) are important to



**Figure 1.** Intramolecular deprotonation of bound H<sub>2</sub>.

the function of many types of hydrogenation catalysts and the family of hydrogenase enzymes.<sup>5,6</sup> A detailed understanding of the heterolysis of a nonpolar bond would greatly inform the design of systems based on heterolytic activation. Here we report an extremely facile, *reversible* heterolytic cleavage of the H–H bond in a Mn complex, wherein the proton and hydride ion undergo exchange through an energetically accessible Mn( $\eta^2$ -H<sub>2</sub>)<sup>+</sup> intermediate at an estimated rate of >10<sup>7</sup> s<sup>-1</sup> at 25 °C.

To mimic a salient feature in the active sites of hydrogenase enzymes,<sup>7</sup> pendant amine bases have been incorporated into families of Ni, Co, and Fe complexes, and their electrochemical behavior under acidic and basic conditions has been studied. This has led to the development of catalysts for H<sub>2</sub> production and oxidation using inexpensive, abundant transition metals rather than precious metals such as platinum.<sup>8</sup> Exploiting a large variety of metal complexes with varying coordination

environments and oxidation states allows for multiple means of controlling the catalytic rate and overpotential. We previously studied cationic Mn(I) complexes containing pendant amines and found that the stable Mn( $\eta^2$ -H<sub>2</sub>)<sup>+</sup> adducts showed no evidence for heterolytic cleavage of H<sub>2</sub>.<sup>9</sup> Reasoning that the acidity of the H<sub>2</sub> ligand in our previous complexes was insufficient to lead to heterolysis, we found in the present work that incorporation of an electron-deficient diphosphine ligand into a new Mn complex (Figure 2) increased the electrophilicity at Mn, facilitating rapid, reversible heterolytic cleavage of H<sub>2</sub>.

The cationic complex **1** (Figure 2) was prepared by halide abstraction from (P<sub>2</sub><sup>Ph</sup>N<sub>2</sub><sup>Bn</sup>)Mn(Br)(CO)(bppm) [bppm =

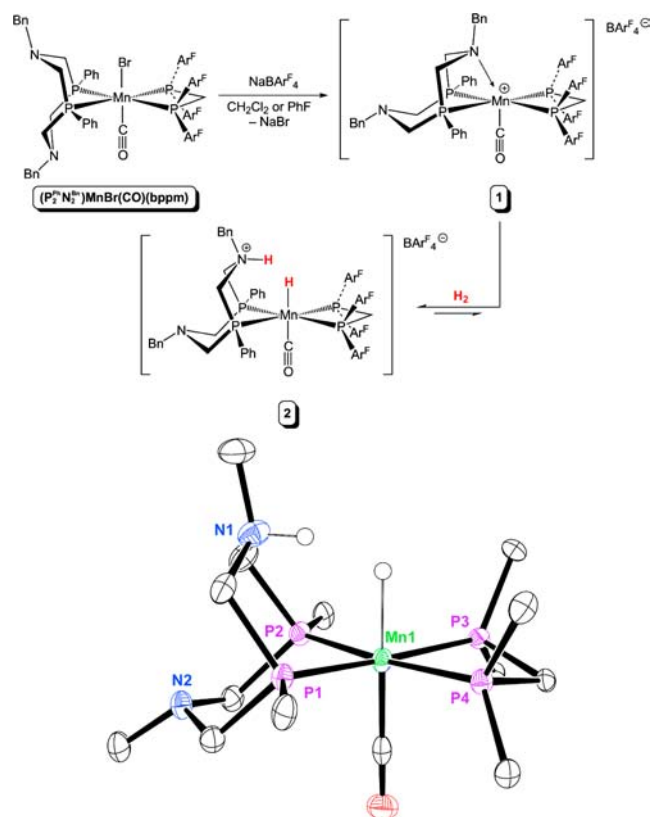


**Figure 2.** Syntheses of [( $\kappa^3$ -P<sup>Ph</sup>N<sup>Bn</sup>)Mn(CO)(bppm)][BAR<sub>4</sub><sup>F</sup>]<sup>+</sup> (**1**) and [(P<sub>2</sub><sup>Ph</sup>N<sub>2</sub><sup>Bn</sup> H)MnH(CO)(bppm)][BAR<sub>4</sub><sup>F</sup>]<sup>+</sup> (**2**) and the truncated solid-state structure of the cation of **2** (–123 °C, 50% probability ellipsoids).

Received: June 8, 2013

Published: July 26, 2013

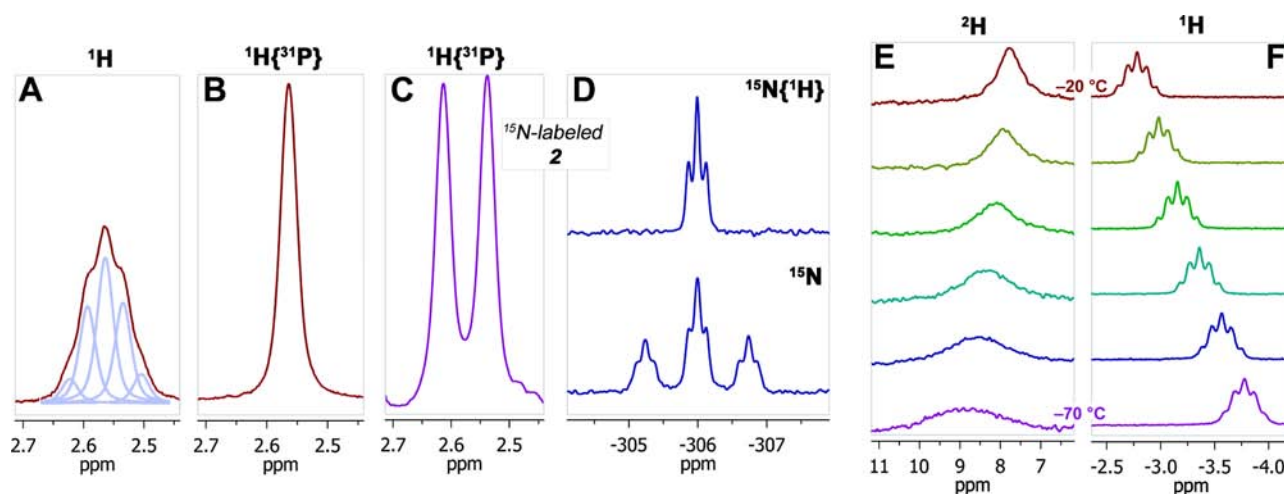


**Figure 3.** Selected regions of (A)  $^1\text{H}$  (with deconvolution) and (B)  $^1\text{H}\{^{31}\text{P}\}$  NMR spectra of **2**; (C)  $^1\text{H}\{^{31}\text{P}\}$ , (D, top)  $^{15}\text{N}\{^1\text{H}\}$ , and (D, bottom)  $^{15}\text{N}$  NMR spectra of  $2\text{-}^{15}\text{N}$ ; and (E)  $^2\text{H}$  and (F)  $^1\text{H}$  NMR spectra of  $2\text{-(H/D)}$  from  $-20$  to  $-70$   $^\circ\text{C}$ .

( $\text{PAr}^{\text{F}}_2$ ) $_2\text{CH}_2$ ;  $\text{Ar}^{\text{F}} = 3,5\text{-bis(trifluoromethyl)phenyl}$  through treatment with excess  $\text{NaBAr}^{\text{F}}_4$  in fluorobenzene. While similar Mn cations previously prepared by Kubas and co-workers are intensely blue,<sup>10</sup> **1** is red-orange as a result of coordination of one of the pendant amines to the Mn center [Figure S1 in the Supporting Information (SI)]. The  $^{31}\text{P}$  NMR resonance for the  $\text{P}_2\text{N}_2$  ligand of **1** was broad at room temperature (Figure S2B), consistent with dynamic behavior related to reversible dissociation of the coordinated pendant amine.

Addition of  $\text{H}_2$  (1 atm) to **1** in PhF or  $\text{CD}_2\text{Cl}_2$  at  $-20$   $^\circ\text{C}$  resulted in a color change from red to yellow and the formation of a single new product (see the  $^{31}\text{P}$  NMR spectrum in Figure S3). Yellow-orange crystals of **2** were grown from  $\text{CH}_2\text{Cl}_2$  solutions under  $\text{H}_2$ , and the solid-state molecular structure determined by X-ray diffraction (Figure 2) is consistent with a static structure containing Mn–H and N–H bonds resulting from heterolytic cleavage of  $\text{H}_2$ .<sup>11</sup>

Spectral studies of **2** in solution indicated dynamic behavior. Besides the expected resonances from ligand protons, the  $^1\text{H}$  NMR spectrum of **2** in  $\text{CD}_2\text{Cl}_2$  exhibited a pseudopentet ( $J_{\text{PH}} \approx 15$  Hz, 2H) at 2.55 ppm that collapsed to a broad singlet upon broadband  $^{31}\text{P}$  decoupling (Figure 3A, B). The modest  $^{31}\text{P}$  coupling [not observed in similar  $\text{Mn}(\eta^2\text{-H}_2)^+$  complexes<sup>9,10</sup>] and the unusual chemical shift are inconsistent with those of  $\text{Mn}(\eta^2\text{-H}_2)^+$  (typically  $-2$  to  $-5$  ppm)<sup>9</sup> or a static structure containing a Mn–H bond (typically  $-4.5$  to  $-6$  ppm)<sup>11</sup> and a N–H bond in the protonated  $\text{P}_2\text{N}_2$  ligand (14 to 7 ppm). When  $\text{D}_2$  was used to produce  $2\text{-(D/D)}$ , the  $^1\text{H}$  NMR spectrum was identical to that of **2** except for the absence of the peak at 2.55 ppm, and the  $^2\text{H}$  NMR spectrum contained a singlet at 2.5 ppm (Figure S4). The existence of a single  $^1\text{H}$  NMR resonance attributable to the Mn–H and N–H positions indicated that those moieties are in rapid exchange, and further isotopic labeling studies supported this conclusion.

In the  $^1\text{H}$  NMR spectrum of the  $^{15}\text{N}$ -labeled analogue  $2\text{-}^{15}\text{N}$  prepared from  $1\text{-}^{15}\text{N}$  and  $\text{H}_2$ , the Mn–H/N–H resonance appeared as a doublet of pentets that collapsed to a doublet upon broadband  $^{31}\text{P}$  decoupling ( $J_{\text{NH}} = 37$  Hz; Figure 3C). The  $^{15}\text{N}$  nucleus coupled to the Mn–H/N–H resonance (assigned by  $^1\text{H},^{15}\text{N}$ -HSQCAD) appeared as a triplet of triplets in the  $^{15}\text{N}$  NMR spectrum ( $J_{\text{NP}} = 7.4$  Hz,  $J_{\text{NH}} = 37$  Hz; Figure 3D), indicating coupling between this  $^{15}\text{N}$  nucleus and two dynamically equivalent protons. The magnitude of  $J_{\text{NH}}$  is

consistent with rapid proton–hydride exchange that results in the observation of an average coupling constant for a “normal”  $^1J_{\text{NH}}$  ( $\sim 70$  Hz)<sup>12</sup> from the protonated amine and negligible  $^{15}\text{N}$  coupling ( $J_{\text{NH}} \approx 0$  Hz) to the hydride ligand. Similarly, the magnitude of  $J_{\text{PH}}$  is approximately half of the value expected for manganese hydrides in this structural family ( $^2J_{\text{PH}} = 15$  Hz observed vs 30–40 Hz expected).<sup>11</sup>

Addition of HD to a  $\text{CH}_2\text{Cl}_2$  solution of **1** at  $-20$   $^\circ\text{C}$  resulted in the observation of an  $^1\text{H}$  NMR spectrum containing resonances identical to those of **2** except for the absence of a peak near 2.5 ppm. Instead, a signal integrating to one proton was observed at  $-2.78$  ppm that appeared as a pseudopentet ( $J_{\text{PH}} = 28$  Hz) and collapsed to a singlet upon broadband  $^{31}\text{P}$  decoupling. The  $^2\text{H}$  NMR spectrum of the same sample revealed only a resonance at  $+7.8$  ppm. In the variable-temperature  $^2\text{H}$  and  $^1\text{H}$  NMR spectra of  $2\text{-(H/D)}$  from  $-20$  to  $-70$   $^\circ\text{C}$  (Figure 3E,F), both the  $^1\text{H}$  and  $^2\text{H}$  chemical shifts showed a strong temperature dependence, linearly shifting by  $>1$  ppm in opposite directions (upfield and downfield, respectively, with decreasing temperature) over a 50  $^\circ\text{C}$  range. The average of these chemical shifts in the  $^1\text{H}$  and  $^2\text{H}$  NMR spectra was 2.5 ppm, consistent with a dynamic process involving rapid exchange of H and D between the amine and metal sites, with a preference for D at the amine and the H at the metal.<sup>13</sup> Although the  $^2\text{H}$  signal became too broad below  $-70$   $^\circ\text{C}$  to allow the chemical shift to be quantified reliably, the  $^1\text{H}$  signal continued to shift consistently upfield, reaching  $-4.32$  ppm at a temperature of  $-94$   $^\circ\text{C}$  (Figure S5).

The assignment of the resonance at 2.55 ppm in the  $^1\text{H}$  NMR spectrum of **2** to rapidly exchanging proton and hydride resonances is thus consistent with the observed average chemical shift, the magnitudes of  $^1J_{\text{NH}}$  and  $^2J_{\text{PH}}$ , and the coupling of two hydrogen atoms to the corresponding  $^{15}\text{N}$  nucleus in the  $^{15}\text{N}$ -labeled complex. Furthermore, the variable-temperature behavior of  $2\text{-(H/D)}$  is expected in the rapid exchange limit. The large opposing changes in the chemical shifts of the  $^1\text{H}$  and  $^2\text{H}$  signals of  $2\text{-(H/D)}$  as the temperature was varied are indicative of an equilibrium isotope effect (EIE) wherein D preferentially resides at the amine while H is bound to Mn.<sup>14</sup>

The magnitude of the preference for N–D over N–H increased at lower temperatures, consistent with the expected

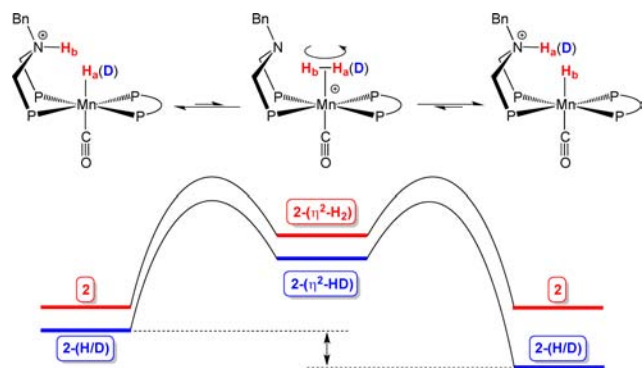


**Figure 4.** Qualitative energy diagram for exchange of the proton and hydride sites of **2** via  $2-(\eta^2\text{-H}_2)$  (red) and a depiction of the effect of isotopic substitution.

influence of the zero-point energy (ZPE) differences in the Mn–(H/D) and N–(H/D) bonds (Figure 4). ZPE differences are expected to dominate this equilibrium (Figure S6), in contrast to other systems such as  $[\text{M}(\text{H})(\text{H}_2)]$  studied by Heinekey and others,<sup>15,16</sup> for which the EIEs may have additional contributions.<sup>14</sup> Those systems can also facilitate rapid  $\text{H}_2$  activation, but the nature of the activation is quite different from that in the present system.<sup>16b</sup>

The temperature dependence of the chemical shifts in  $2-(\text{H}/\text{D})$  is entirely due to thermodynamics: for the chemical shifts to reflect weighted averages of the different isotopomers, exchange must be fast on the NMR time scale. Assuming the chemical shift of the static hydride in  $2-(\text{H}/\text{D})$  to be between  $-4.5$  and  $-5.5$  ppm, we estimate that the EIE for  $2-(\text{MnH}/\text{ND}) \rightleftharpoons 2-(\text{MnD}/\text{NH})$  is in the range  $0.13$ – $0.23$  at  $-20$  °C.<sup>11</sup> An intramolecular EIE of similar magnitude ( $K = 0.41$  at  $56$  °C) was observed by Toomey et al.<sup>17</sup> in the amido hydride  $(\eta^2\text{-C}_5(\text{CH}_3)_4\text{H})_2\text{Zr}(\text{H}/\text{D})(\text{N}(\text{D}/\text{H})^t\text{Bu})$ , wherein slow intramolecular H/D exchange facilitated an equilibrium favoring the  $[\text{Zr}(\text{H})][\text{N}(\text{D})^t\text{Bu}]$  isotopomer.

The rate of the  $\text{H}^+/\text{H}^-$  interconversion in **2** is related to the difference in the frequencies of the two resonances that are being averaged, but the isolated chemical shifts could not be established by “freezing out” the dynamism. In the  $^1\text{H}$  NMR spectra of **2** from  $-25$  to  $-95$  °C, the proton–hydride resonance remained coalesced over the entire temperature range (Figure S7A), and similarly, the  $^2\text{H}$  NMR spectrum of  $2-(\text{D}/\text{D})$  remained coalesced down to  $-90$  °C (Figure S7B). The  $^1\text{H}$  NMR spectra of **2** did show appreciable broadening of the Mn–H/N–H resonance as the temperature was lowered, but concomitant broadening of ligand and solvent resonances suggested that this was due to ion-pair formation and/or an increase in solution viscosity. On the basis of the lowest measured  $^1\text{H}$  chemical shift of  $2-(\text{H}/\text{D})$  ( $-4.32$  ppm) and the known averaged chemical shift of **2** ( $2.55$  ppm), we estimate a minimum N–H/Mn–H peak separation of  $13.7$  ppm, corresponding to a reversible heterolytic  $\text{H}_2$  cleavage rate greater than  $1.5 \times 10^4$   $\text{s}^{-1}$  at  $-95$  °C. This minimum rate is consistent with a  $\Delta G^\ddagger$  of less than  $6.8$  kcal/mol for the overall exchange process. If a similar barrier at room temperature is assumed,  $\text{H}^+/\text{H}^-$  exchange occurs at a rate of at least  $10^7$   $\text{s}^{-1}$  at  $25$  °C.<sup>11,18</sup> There are several previous examples of directly observed  $\text{H}^+/\text{H}^-$  exchange,<sup>19</sup> although they occur at substantially lower rates, and others where exchange is implied as part of an overall process.<sup>20</sup>

The Mn–H and N–H sites are proposed to exchange through an energetically accessible  $\text{Mn}(\eta^2\text{-H}_2)^+$  complex. Exchange between dissolved  $\text{H}_2$  and **2** was shown by exchange spectroscopy (EXSY) experiments, which revealed that the Mn–H/N–H resonance was in chemical exchange with free  $\text{H}_2$  at an approximate rate of  $0.1$ – $10$   $\text{s}^{-1}$  at  $25$  °C (Figure S8). Moreover, addition of  $\text{H}_2$  to **1** was only slightly favorable at  $1$  atm [ $\Delta G = -2.1(3)$  kcal  $\text{mol}^{-1}$ ],<sup>11</sup> and removal of the  $\text{H}_2$  atmosphere at  $20$  °C resulted in complete conversion back to red-orange **1** as rapidly as the solution could be degassed. Since no significant HD coupling was observed in  $2-(\text{H}/\text{D})$  (expected  $J_{\text{HD}} \sim 30$  Hz for an  $\eta^2\text{-HD}$  complex),<sup>15,21</sup> the complex  $2-(\eta^2\text{-HD})$  likely lies at least  $1$  kcal  $\text{mol}^{-1}$  above  $2-(\text{H}/\text{D})$ . On the basis of this result and the negligible temperature dependence of the  $^1\text{H}$  NMR chemical shifts of **2**, the intermediate  $2-(\eta^2\text{-H}_2)$  likely also lies at least  $1$  kcal  $\text{mol}^{-1}$  above **2**. Because of the higher energy of  $2-(\eta^2\text{-H}_2)$  relative to **2**, the barrier for heterolytic cleavage of  $\text{H}_2$  in this intermediate is correspondingly lower than that for the overall exchange process between the proton and hydride sites in **2** (i.e.,  $\Delta G^\ddagger \leq 5.8$  kcal  $\text{mol}^{-1}$  for  $\text{H}_2$  cleavage). Moreover, the temperature dependence of the  $^1\text{H}$  NMR signal of  $2-(\text{H}/\text{D})$ , indicative of the EIE and thus still rapid  $\text{H}^+/\text{H}^-$  exchange, did not show a deviation that would indicate a kinetic isotope effect (KIE). Since a significant primary KIE would be expected for an event involving substantial H–H bond breaking/making, this suggests that the minimum  $\text{H}^+/\text{H}^-$  exchange rate of  $1.5 \times 10^4$   $\text{s}^{-1}$  at  $-95$  °C may be a considerable underestimate.

Observation of the extremely rapid, reversible heterolytic cleavage of  $\text{H}_2$  into a proton and a hydride ion in this bifunctional manganese complex may give insight into synthetic catalysts and enzymes that heterolytically cleave  $\text{H}_2$ . Energy matching between the heterolytic cleavage product and the  $\text{Mn}(\eta^2\text{-H}_2)^+$  complex was obtained, such that exchange between the Mn–H and N–H sites was facile. The rate of the overall exchange has been estimated to be  $>10^7$   $\text{s}^{-1}$  at  $25$  °C, which is orders of magnitude higher than the rates of catalysis for  $\text{H}_2$  oxidation or production in  $[\text{FeFe}]$  hydrogenase<sup>5</sup> and reported molecular catalysts that mimic the function of this enzyme.<sup>22</sup> The facility of  $\text{H}_2$  activation shown here suggests that other suitably energy-matched systems may be able to perform facile heterolysis of nonpolar substrates, an as-yet underutilized strategy in the activation of, for example, alkane C–H bonds.

## ■ ASSOCIATED CONTENT

### 📄 Supporting Information

Experimental procedures, syntheses, and X-ray crystallographic data (CIF). This material is available free of charge via the Internet at <http://pubs.acs.org>.

## ■ AUTHOR INFORMATION

### Corresponding Author

[morris.bullock@pnml.gov](mailto:morris.bullock@pnml.gov)

### Notes

The authors declare no competing financial interest.

## ■ ACKNOWLEDGMENTS

We are grateful to Dr. Monte Helm for assistance in revising this manuscript. We thank the U.S. Department of Energy, Office of Basic Energy Sciences, Division of Chemical Sciences, Geosciences and Biosciences, for support of the initial parts of

this work. The current work was supported by the Center for Molecular Electrocatalysis, an Energy Frontier Research Center funded by the U.S. Department of Energy, Office of Science, Office of Basic Energy Sciences. Pacific Northwest National Laboratory is operated by Battelle for the U.S. Department of Energy.

## REFERENCES

- (1) DuBois, D. L.; Bullock, R. M. *Eur. J. Inorg. Chem.* **2011**, 1017.
- (2) Ogo, S. *Chem. Commun.* **2009**, 3317.
- (3) (a) Noyori, R.; Yamakawa, M.; Hashiguchi, S. *J. Org. Chem.* **2001**, 66, 7931. (b) Abdur-Rashid, K.; Clapham, S. E.; Hadzovic, A.; Harvey, J. N.; Lough, A. J.; Morris, R. H. *J. Am. Chem. Soc.* **2002**, 124, 15104.
- (c) de Vries, J. G.; Elsevier, C. J. *Handbook of Homogeneous Hydrogenation*; Wiley-VCH: Weinheim, Germany, 2007.
- (4) Wayner, D. D. M.; Parker, V. D. *Acc. Chem. Res.* **1993**, 26, 287.
- (5) Frey, M. *ChemBioChem* **2002**, 3, 153.
- (6) Fontecilla-Camps, J. C.; Volbeda, A.; Cavazza, C.; Nicolet, Y. *Chem. Rev.* **2007**, 107, 4273.
- (7) (a) Cracknell, J. A.; Vincent, K. A.; Armstrong, F. A. *Chem. Rev.* **2008**, 108, 2439. (b) Tard, C.; Pickett, C. J. *Chem. Rev.* **2009**, 109, 2245.
- (8) (a) Rakowski DuBois, M.; DuBois, D. L. In *Catalysis Without Precious Metals*; Bullock, R. M., Ed.; Wiley-VCH: Weinheim, Germany, 2010. (b) Camara, J. M.; Rauchfuss, T. B. *Nat. Chem.* **2012**, 4, 26. (c) Singleton, M. L.; Crouthers, D. J.; Duttweiler, R. P., III; Reibenspies, J. H.; Darensbourg, M. Y. *Inorg. Chem.* **2011**, 50, 5015. (d) Tard, C.; Liu, X.; Ibrahim, S. K.; Bruschi, M.; De Gioia, L.; Davies, S. C.; Yang, X.; Wang, L.-S.; Sawers, G.; Pickett, C. J. *Nature* **2005**, 433, 610. (e) Lounissi, S.; Zampella, G.; Capon, J. F.; De Gioia, L.; Matoussi, F.; Mahfoudhi, S.; Petillon, F. Y.; Schollhammer, P.; Talarmin, J. *Chem.—Eur. J.* **2012**, 18, 11123. (f) Liu, T.; DuBois, D. L.; Bullock, R. M. *Nat. Chem.* **2013**, 5, 228.
- (9) Welch, K. D.; Dougherty, W. G.; Kassel, W. S.; DuBois, D. L.; Bullock, R. M. *Organometallics* **2010**, 29, 4532.
- (10) King, W. A.; Luo, X.-L.; Scott, B. L.; Kubas, G. J.; Zilm, K. W. *J. Am. Chem. Soc.* **1996**, 118, 6782.
- (11) See the SI for additional details.
- (12) Wilson, A. D.; Shoemaker, R. K.; Miedaner, A.; Muckerman, J. T.; DuBois, D. L.; Rakowski DuBois, M. *Proc. Natl. Acad. Sci. U.S.A.* **2007**, 104, 6951.
- (13) Calvert, R. B.; Shapley, J. R. *J. Am. Chem. Soc.* **1978**, 100, 7726.
- (14) (a) Parkin, G. *Acc. Chem. Res.* **2009**, 42, 315. (b) Bullock, R. M.; Bender, B. R. In *Encyclopedia of Catalysis*; Horváth, I., Ed.; Wiley: New York, 2002; Vol. 4, pp 281–348.
- (15) Heinekey, D. M.; Oldham, W. J., Jr. *Chem. Rev.* **1993**, 93, 913.
- (16) (a) Oldham, W. J., Jr.; Hinkle, A. S.; Heinekey, D. M. *J. Am. Chem. Soc.* **1997**, 119, 11028. (b) Maseras, F.; Lledós, A.; Clot, E.; Eisenstein, O. *Chem. Rev.* **2000**, 100, 601.
- (17) Toomey, H. E.; Pun, D.; Veiros, L. F.; Chirik, P. J. *Organometallics* **2008**, 27, 872.
- (18) Calculated from the Eyring equation using  $\Delta G^\ddagger = 6.8$  kcal mol<sup>-1</sup> (see the SI for additional details).
- (19) (a) Lee, J. C., Jr.; Peris, E.; Rheingold, A. L.; Crabtree, R. H. *J. Am. Chem. Soc.* **1994**, 116, 11014. (b) Caballero, A.; Jalón, F. A.; Manzano, B. R. *Chem. Commun.* **1998**, 1879.
- (20) (a) Lough, A. J.; Park, S.; Ramachandran, R.; Morris, R. H. *J. Am. Chem. Soc.* **1994**, 116, 8356. (b) Chu, H. S.; Lau, C. P.; Wong, K. Y.; Wong, W. T. *Organometallics* **1998**, 17, 2768.
- (21) Addition of HD to [(P<sup>Ph</sup>N<sup>Bn</sup>)Mn(CO)(dppm)][BAR<sup>F</sup><sub>4</sub>] (the dppm analogue of **2**; see ref 9) yielded a “normal”  $\eta^2$ -HD adduct [<sup>1</sup>H NMR (500 MHz, PhF) of  $\eta^2$ -HD:  $\delta$  -3.00 ppm,  $J_{\text{HD}} = 32$  Hz].
- (22) Helm, M. L.; Stewart, M. P.; Bullock, R. M.; Rakowski DuBois, M.; DuBois, D. L. *Science* **2011**, 333, 863.